Numerical solution of stochastic partial differential systems with additive noise on overlapping subdomains

Mostafa Zahri

College of Sciences, Department of Mathematics, Research Group MASEP
University of Sharjah, United Arab Emirates
e-mail: mzahri@sharjah.ac.ae

June 29, 2019

Abstract. *In this paper, we present a new numerical approach for solving a class of stochastic partial differential systems with additive noise on overlapping subdomains. We combine the domain decomposition method, the deterministic method of lines and the barycentric interpolation method. In addition to the combination of these three methods, we implement the stochastic Itô-Taylor family schemes for solving a stochastic advection-diffusion-reaction problems. The solution of the stochastic system is then carried out by collecting interior and interface solutions. Finally, computational results are performed on two dimensional overlapped subdomains with nonlinear boundaries.*

Keywords: Domain-decomposition, Schwarz method, Itô-Taylor, barycentric interpolation, stochastic advection-diffusion, overlapping subdomains, interface solution.

AMS Subject Classifications: *35K57, 35R60, 60H15, 60H35*

1 Motivation

The Domain decomposition methods (DDM) for solving evolutionary partial differential equations (PDEs) was first introduced by Schwarz [19]. This classical alternating Schwarz method (ASM) is used to approximate PDEs solutions on an overlapped circle and rectangle. Where the used scheme solves the problem on the circle with boundary condition taken from the interior of the rectangle and solves the PDEs on the rectangle with boundary condition taken from the interior of the circle. The DDM techniques deal in general with solving subproblems on subdomains instead of solving the initial problem on a computational domain without decomposition. The solution of these subproblems is qualitatively or quantitatively simpler than the original problem [20, 21, 22, 30]. In the framework of numerical analysis for PDEs, the DDM solves a boundary value problem by splitting it into smaller boundary value problems on several subdomains. Generally, these problems on the subdomains are independent, which makes the domain decomposition methods suitable for parallel computing [3, 14, 15, 16]. These techniques are typically used as preconditioners for Krylov space iterative methods, such as the conjugate gradient

method or Generalized minimal residual method (GMRES) [28, 31]. Later, Lions in [9, 10] extends the ASM to more suitable algorithm. He proposed an interesting additive Schwarz method. The overlapping DDM, which include the alternating and the additive Schwarz method, is the concern, where the subdomains overlap by more than the interface. Moreover, they could be written and analyzed as special cases of the abstract additive Schwarz method.

In this work, we transform the Schwarz algorithm for solving stochastic partial differential equations (SPDEs) on overlapping subdomains into an equivalent problem on non-overlapping subdomains. Where, the concentration on the overlapping region, considered as new function, is a consequence of chemical and physical transformation of those from the non-overlapped subdomains. Thereafter, we solve the system of SPDEs with additive noise using a class of stochastic Itô-Taylor (SIT) schemes [2, 4, 8, 7, 17], combined with the deterministic the method of lines (MOL) [24, 32, 18, 25] and the barycentric interpolation method (BIM) for approximating the interface solutions [34, **?**]. In the present work, similar to the parallel Schwarz Waveform Relaxation Algorithm presented in [12, 13], we analytically construct a new numerical approach for approximating the non-overlapping interface of the overlapping region of the computational domain.

This paper is organized as follows: In Section 2, we introduce overlapping stochastic problem and the corresponding non-overlapping equivalent one. Thereafter, we suggest an algorithm for interpolating the interface solution. In Section 3, we construct the Itô-Taylor family schemes for solving the equivalent system of systems. In Section 4, we present the time-space integration of the problem. While, in Section 5, we accurate our method using several tests. We perform geometrical and numerical experiments on two dimensional subdomains with nonlinear boundaries. Finally, comments and some concluding remarks are presented in Section 6.

2 Modeling of SPDS on decomposed subdomains

In the following section, we present a stochastic overlapped and alternating Schwarz problem. Thereafter, we transform it into a non-overlapping parallel problem. Because of the reactions and actions of species inside the common region, the solution of the PDEs problem on the overlapped interface lead to the introduction of a new function. Moreover, we set up some advantages of the proposed transformation.

2.1 SPDS on overlapping subdomains

Consider a probability space $(\Omega, \mathcal{F}_t, P)$, where Ω denotes the space of outcomes. The sequence $\mathcal{F}_t$ is a family of right continuous filtrations associated with Ω, for all $t \in [0, T]$ with $T > 0$. P is the probability measure on the right continuous $\mathcal{F}_t$. Moreover, denote by $\mathbf{H} = L^2\Big(I\!R^2, I\!R\Big)$ the separable real Hilbert space of square integrable real valued functions defined from $I\!R^2$ to $I\!R$ with scalar product and usual norms. For two overlapping

subdomains D_1 and D_2 such that $D_1 \cap D_2 = \Gamma_{1,2}$, we suppose that $\boldsymbol{U}^s$ is the time-space stochastic processes defined as a mapping $\boldsymbol{U}^s : [0,T] \times D_s \times \Omega \longrightarrow I\!R$, for $s = 1, 2$. Denote by $(\boldsymbol{U}^1, \boldsymbol{U}^2)$ the exact solution of the following stochastic partial differential system:

$$\begin{aligned} \boldsymbol{U}_t^1 &= \nabla \cdot (d_1 \nabla \boldsymbol{U}^1) - a_1 \cdot \nabla \boldsymbol{U}^1 + \sigma^1 \eta^1, \quad \text{on} \quad \boldsymbol{D}_1, \\ \boldsymbol{U}_t^2 &= \nabla \cdot (d_2 \nabla \boldsymbol{U}^2) - a_2 \cdot \nabla \boldsymbol{U}^2 + \sigma^2 \eta^2, \quad \text{on} \quad \boldsymbol{D}_2, \end{aligned} \tag{1}$$

where, for $s = 1, 2$ the processes η^s are two independent white noises. The parameters σ^s are two standard correlations, d_s are a constant diffusion coefficients and a_s represent a constant advection parameters. the time-space processes $\boldsymbol{U}^s$ could be interpreted as densities of interacting species X and Y respectively, see for instance similar works in [1, 24]. In order to numerically solve the problem (1), other factors should be be taken in consideration. Namely, the evolution of the species X and Y on the overlapped subdomain $\Gamma_{1,2}$. Therefore, we suggest the following classical chemical reactions:

$$X \longrightarrow \alpha_t X + (1 - \alpha_t) X, \tag{2}$$

$$Y \longrightarrow (1 - \alpha_t) Y + \alpha_t Y, \tag{3}$$

$$\alpha_t X + (1 - \alpha_t) Y \longrightarrow XY, \tag{4}$$

where for all $t \in [0, T]$, α_t is chosen as a deterministic or as a random variable with outcomes in the real interval $[0, 1]$. The reactions (2) and (3) refers the molecular decomposition, where larger molecule splits into smaller parts. The reaction (4) is of types bimolecular reactions. For instance when two molecules $\alpha_t X$ and $(1 - \alpha_t)Y$ collide and react with each other. Hence, let us denotes by $\boldsymbol{U}^3$ the density function of the new chemical product XY on the overlapping subdomain $\Gamma_{1,2}$. It satisfies the following physical and chemical splitting transformation:

$$\begin{cases} \boldsymbol{U}^1 \longrightarrow (1 - \alpha_t)\boldsymbol{U}^1 & \text{on} \quad \boldsymbol{D}_1 \setminus \Gamma_{1,2}, \\ \boldsymbol{U}^2 \longrightarrow \alpha_t \boldsymbol{U}^2 & \text{on} \quad \boldsymbol{D}_2 \setminus \Gamma_{1,2}, \\ \alpha_t \boldsymbol{U}^1 + (1 - \alpha_t)\boldsymbol{U}^2 \longrightarrow \boldsymbol{U}^3 & \text{on} \quad \Gamma_{1,2}. \end{cases} \tag{5}$$

Therefore, a new numerical approach is required for solving the SPDS (1) on D together with (5) on the overlapping subdomain $\Gamma_{1,2}$. For the time-space integration, we use the parallel domain decomposition algorithm (DDA) and we apply the method of lines (MOL) to transform the SPDS (1) into a semi-linear system of systems with random entries, see [24, 32]. We solve these systems locally on $D_1 \setminus \Gamma_{1,2}$, on $D_2 \setminus \Gamma_{1,2}$ and we update the solution on the boundary of the interface $\Gamma_{1,2}$. For continuity purposes of the solution on all common interfaces Γ_u and Γ_d, see figure 1, we force α_t to be temporal and spatial function.

2.2 Non-overlapping equivalent problem

In this section, we introduce an non-overlapping equivalent problem for solving the overlapping SPDS (1) together with (5). In fact, to deal with this problem, we have to solve $\boldsymbol{U}^1$ on $\boldsymbol{D}_1 \setminus \Gamma_{1,2}$, $\boldsymbol{U}^2$ on $\boldsymbol{D}_2 \setminus \Gamma_{1,2}$ and solving a new SPDE problem for $\boldsymbol{U}^3$ on $\Gamma_{1,2}$. Unlike the alternating deterministic Schwarz algorithm [19, 9, 10], we solve the system (1) using the parallel Schwarz scheme, by introducing the new function $\boldsymbol{U}^3$ and taking in consideration the changes inside the overlapping subdomain. Hence, due to the reactional changes on the overlapping region, the new reactional equation is given by

$$\boldsymbol{U}_t^3 = \nabla \cdot (f(d_1, d_2)\nabla \boldsymbol{U}^3) - g(a_1, a_2) \cdot \nabla \boldsymbol{U}^3 + \sigma^1 \eta^1 + \sigma^2 \eta^2, \tag{6}$$

where the variable $\alpha_t(\omega)$ have outcomes in $[0, 1]$, the diffusion coefficient $d_3 = f(d_1, d_2)$ is a function of d_1 and d_2, the advection coefficient $a_3 = g(a_1, a_2)$ is a function of the advection a_1 and a_2. Finally, the resulting overlapping equivalent problem has the form:

$$\begin{cases} \boldsymbol{U}_t^1 &= d_1 \Delta \boldsymbol{U}^1 - a_1 \nabla \boldsymbol{U}^1 + \sigma^1 \eta^1 & \text{on} \quad \boldsymbol{D}_1 \setminus \Gamma_{1,2}, \\ \boldsymbol{U}_t^2 &= d_2 \Delta \boldsymbol{U}^2 - a_2 \nabla \boldsymbol{U}^2 + \sigma^2 \eta^2 & \text{on} \quad \boldsymbol{D}_2 \setminus \Gamma_{1,2}, \\ \boldsymbol{U}_t^3 &= d_3 \Delta \boldsymbol{U}^3 - a_3 \nabla \boldsymbol{U}^3 + \sigma^1 \eta^1 + \sigma^2 \eta^2 & \text{on} \quad \Gamma_{1,2} \end{cases} \tag{7}$$

In order to complete the transformation above to numerically solve the original domain decomposition problem, we have to approximate the local solutions $\boldsymbol{U}^1$, $\boldsymbol{U}^2$ and $\boldsymbol{U}^3$ on $\partial\Gamma_{1,2} = \Gamma_u \cup \Gamma_d$, see Figure (1).

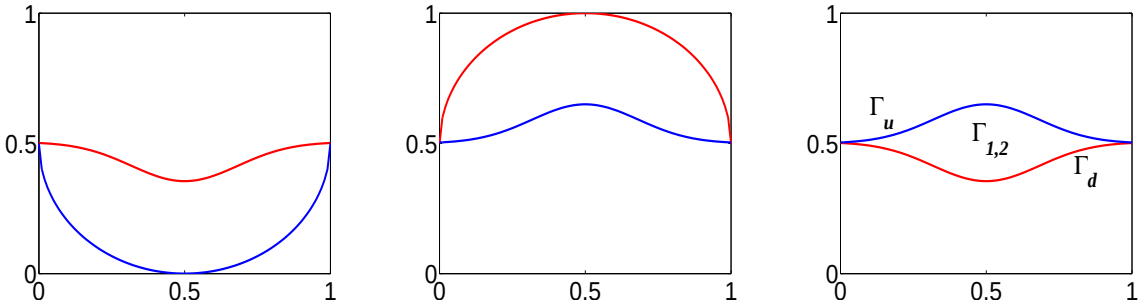

(a) $D_1 \setminus \Gamma_{1,2}$ (b) $D_2 \setminus \Gamma_{1,2}$ (c) Interface $\Gamma_{1,2}$

Figure 1: Computational Domains.

The interface solution should satisfy the following boundary conditions:

$$\begin{cases} \mathbf{w}^{1,3} &= \boldsymbol{U}_t^3 = \boldsymbol{U}_t^1 \quad \text{on} \quad \Gamma_d, \\ \mathbf{w}^{2,3} &= \boldsymbol{U}_t^3 = \boldsymbol{U}_t^2 \quad \text{on} \quad \Gamma_u, \end{cases} \tag{8}$$

where the interface solutions $\mathbf{w}^{1,3}$ and $\mathbf{w}^{2,3}$ are approximated using the barycentric interpolation method (13) presented in the next section. For more details, we also refer to [34, **?**].

2.3 Interpolation of the interface solution

In order to construct the interface solutions $\mathbf{w}$, we use the FTCS-BIM scheme, see [5, 6, 34, **?**]. For the non-overlapping interfaces Γ_u and Γ_d and a given time FTCS discretization of the problem (8), we define the neighbors grid-points index set $N_{i,j}^m$ as

$$N_{i,j}^m := \Big\{(i+a, j+b)\Big||a| = |b| = m; a, b \in \mathbb{Z}\Big\}. \tag{9}$$

We define, the coefficients set $\alpha_{i^*,j^*} \in C_{i,j} \subset]0,1[$ as

$$\begin{aligned} C_{i,j} \;:=\; & \Big\{\big(\frac{1-2\alpha}{4}\big)_{i+2,j-2}, \big(\frac{1-2\alpha}{4}\big)_{i+2,j+2}, \big(\frac{\alpha}{2}\big)_{i+1,j-1}, \big(\frac{\alpha}{2}\beta^-\big)_{i+1,j+1}, \\ & \big(\frac{1-2\alpha}{4}\big)_{i-2,j-2}, \big(\frac{1-2\alpha}{4}\big)_{i-2,j+2}, \big(\frac{\alpha}{2}\beta^+\big)_{i-1,j-1}, \big(\frac{\alpha}{2}\big)_{i-1,j+1}\Big\}. \end{aligned}$$

and satisfies the following convex combination

$$\sum_{\alpha_{i^*,j^*} \in C_{i,j}} \alpha_{i^*,j^*} = \sum_{(i^*,j^*) \in N_{i,j}^1 \cup N_{i,j}^2} \alpha_{i^*,j^*} = 1. \tag{10}$$

where the notation α, β^+ and β^- stand for

$$\alpha = \frac{2d\Delta t}{(\Delta x)^2}, \qquad \beta^- = 1 - \frac{a}{2d}\Delta x, \quad \text{and} \quad \beta^+ = 1 + \frac{a}{2d}\Delta x. \tag{11}$$

For more details about the construction of this method, we refer to [**?**].

Under appropriate conditions on initial solution $\boldsymbol{U}^0$ in $L^2(\boldsymbol{D})$, there exist a unique solution $\boldsymbol{U}^{DD}$ in $C([0,T], L^2(\boldsymbol{D})) \cap L^2(0,T; H_0^1(\boldsymbol{D}))$, such that the DDM solution

$$\boldsymbol{U}^{DD}(\mathbf{x},t) \;:=\; \mathbf{w}(\mathbf{x},t)\big|_{\partial\Gamma_{1,2}} + \sum_{s=1}^{3} \boldsymbol{U}^s(\mathbf{x},t)\big|_{\boldsymbol{D}_s \setminus \partial \boldsymbol{D}_s}, \tag{12}$$

where $\boldsymbol{U}^s$ is the solution of the sub-problem s for $s = 1, 2, 3$ and the mapping $\mathbf{w}(\mathbf{x}, t)$ is the whole interface solution. This non-overlapping interface solution is recursively computed as updated function depending on the values of $\boldsymbol{U}$ at $(t - \Delta t)$, which is given by

$$\mathbf{w}(\mathbf{x}_{i,j}) := \begin{cases} \boldsymbol{U}^{DD}(\mathbf{x}_{i,j}, 0) & \text{for} \quad t = 0, \\ \sum\limits_{(i^*,j^*) \in N_{i,j}^1 \cup N_{i,j}^2} \alpha_{i^*,j^*} \boldsymbol{U}^{DD}(\mathbf{x}_{i^*,j^*}, t - \Delta t) & \text{for} \quad t > 0 \end{cases} \tag{13}$$

where

$$\boldsymbol{U}^{DD}(\mathbf{x}_{i,j}, 0) = \boldsymbol{U}^s(\mathbf{x}_{i,j}, 0).$$

The initial and Dirichlet boundary conditions are

$$\begin{aligned} \boldsymbol{U}^s(\mathbf{x},0) &= \boldsymbol{U}(\mathbf{x},0)\big|_{\boldsymbol{D}_s} \quad \text{for} \quad s = 1,2,3. \\ \boldsymbol{U}^s(\mathbf{x},t) &= 0 \qquad\qquad\quad \text{for} \quad (\mathbf{x},t) \in \partial\boldsymbol{D} \times [0,T]. \end{aligned} \tag{14}$$

Consider the deterministic case, where i.e $\sigma^1 = \sigma^2 = 0$. In order to solve the equivalent problem (8) on non-overlapping subdomains, we assume that the following advection and diffusion coefficients hold for any interface point $\mathbf{x}_{i,j} \in \Gamma_u$ or Γ_d:

$$d_3 := \frac{1}{2}(d_1 + d_2) \quad \text{and} \quad a_3 := \frac{1}{2}(a_1 + a_2).$$

Thus, we have the following convergence theorem

Theorem 1. *For $\mathbf{x}_{i,j} \in \Gamma_u$ or Γ_d, if $4d_3\Delta t < (\Delta x)^2$, $\Delta x < 2d_3/a_3$, then there exists a sequence $(\alpha_{i,j})_k$ such that following two step Barycentric scheme*

$$\boldsymbol{U}(\mathbf{x}_{i,j}, t_{n+1}) \approx U_{i,j}^{n+1} = \sum_{(i^*,j^*)\in N_{i,j}^1 \cup N_{i,j}^2} \alpha_{i^*,j^*} \boldsymbol{U}^{DD}(\mathbf{x}_{i^*,j^*}, t_n), \tag{15}$$

approximates $\boldsymbol{U}(\mathbf{x}_{i,j}, t_{n+1})$ in the problem (1) and in the system (8) with time-space convergence order $\mathcal{O}(\Delta t + (\Delta x)^2)$.

For the proof, we refer to [**?**].

3 Itô-Taylor schemes for SPDEs on overlapping subdomains

In this section, we recall the construction of the Itô-Taylor scheme for integrating stochastic differential systems driven by at most two uncorrelated noises. First, we set up some classical definitions and notations, for more details see [34]:

The Component set is an ordered subset, denoted by F_2^0. It contains the whole numbers 0, 1 and 2:

$$F_2^0 := \{0\} \cup F_2 = \{0\} \cup \{1, 2\} = \{0, 1, 2\}.$$

The Multi-index is an ℓ-tuple, denoted by $\alpha = (j_1, \ldots, j_l)$, where $j_i \in F_2^0$ and $1 \leq i \leq l$.

The Length of a Multi-index is the number of components of α, denoted by $\ell(\alpha) := \ell_\alpha$.

The Zeros a multi-index is the number of zero components of α, denoted by $n(\alpha) := n_\alpha$.

The Multi-index set is the set of all multi-indices with respect to F_2, represented by

$$\mathcal{M}_2 = \bigcup_{l=1}^{\infty} (F_2^0)^l \cup \{v\},$$

where v refers to the empty multi-index with size zero.

The drop operator $(-)$ is defined for a multi-index $\alpha = (j_1, j_2, \ldots, j_l) \in \mathcal{M}_2$, such that

$$-\alpha := (j_2, \ldots, j_l) \quad \text{and} \quad \alpha- := (j_1, j_2, \ldots, j_{l-1}).$$

Example 1. The following examples makes clear the definition above:

- For $\alpha = (1, 0)$, we have $\ell(\alpha) = 2$ and $n(\alpha) = 1$.
- For $\alpha = (1, 0, 1)$, we have $\ell(\alpha) = 3$ and $n(\alpha) = 1$.
- For $\alpha = (1, 0, 2)$, we have $-\alpha = (0, 2)$ and $\alpha- = (1, 0)$.
- If $\ell(\alpha) = l = 1$ then $-\alpha = \alpha- = v$ and $l(-\alpha) = l(\alpha-) = 0$.

Throughout the following section, all stochastic processes are defined on a probability space $(\Omega, \mathcal{F}_t, P)$ with right continuous augmented filtration $\mathcal{F}_t, t \in [0, T]$.

Definition 1. Denote by H, the set of stochastic processes $(f_t)_{t\geq 0}$, which are progressively adapted to the associated filtration $\{\mathcal{F}_t\}_{t\geq 0})$, right continuous and the left limit exists. We define the sets $H_v, H_{(0)}, H_{(1)}$ of essentially bounded, integrable and square integrable processes as

(i). $H_v := \{f \in H : \forall\ t \geq t_0 \quad |f(t, w)| < \infty \quad \text{a.s.}\}$,

(ii). $H_{(0)} := \left\{f \in H : \forall\ t \geq t_0 \quad \int_{t_0}^t |f(s, w)|ds < \infty \quad \text{a.s.}\right\}$,

(iii). $H_{(j)} := \left\{f \in H : \forall\ t \geq t_0 \quad \int_{t_0}^t |f(s, w)|^2 ds < \infty \quad \text{a.s.}\right\}$, for $j \in F_2^0$.

where the notation $a.s.$ refers 'almost sure' in the theory of stochastic calculus. Moreover, we assume that the sets $H_{(1)} = H_{(j)}$ coincide, for all $j \in F_2^0$. for more details, we refer to [7, 8].

Definition 2. Consider $\alpha = (j_1, j_2, \ldots, j_l)$ a multi-index and an m-dimensional Brownian motion $(W_t)_{t\geq 0}$. For $f \in H_{(\alpha)}$, multiple Itô-integrals are defined per recursion as follows:

$$I_\alpha[f(.)]_{t_0,t} := \begin{cases} f(t), & \text{if } l = 0, \\ \int_{t_0}^t I_{\alpha-}[f(.)]_{t_0,s} ds, & \text{if } l \geq 1 \text{ and } j_l = 0, \\ \int_{t_0}^t I_{\alpha-}[f(.)]_{t_0,s} dW_s^{j_l}, & \text{if } l \geq 1 \text{ and } j_l \geq 1. \end{cases}$$

Here $H_{(\alpha)}$ is defined per recursion as

$$H_{(\alpha)} := \{f \in H : \quad I_{(\alpha-)}[f(.)]_{t_0,.} \in H_{(j_l)}\}, \tag{16}$$

for $j_l \in F_2$ and $l \geq 2$.

Example 2. We illustrate the Definition above in the following examples

$$\begin{aligned} I_{(1,2)}[f(.)]_{t_0,t} &= \int_{t_0}^t \int_{t_0}^s f(z) dW_z^1 dW_s^2. \\ I_{(1,2,0)}[f(.)]_{t_0,t} &= \int_{t_0}^t I_{(1,2)}[f(.)]_{0,s} ds = \int_{t_0}^t \int_{t_0}^s \int_{t_0}^{s_1} f(s_2) dW_{s_2}^1 dW_{s_1}^2 ds. \\ I_{(1,2,0,1)}[f(.)]_{t_0,t} &= \int_{t_0}^t I_{(1,2,0)}[f(.)]_{0,s} dW_s^1. \end{aligned}$$

For simplicity, we use the following notations $I_{\alpha,t} = I_\alpha[1]_{0,t}$ and $W_t^0 = t$.

In order to integrate the stochastic partial differential system (1), we first introduce the Itô-Taylor scheme for differential systems of equations. Let $(W_t)_{t\in[t_0,T]}$ be an m-dimensional Brownian motion defined on a $(\Omega,\mathcal{A})^2$ with right continuous augmented filtration $\mathcal{F}=(\mathcal{F}_t)_{t\in[0,T]}$. Consider the following d-dimensional Itô process $\boldsymbol{X}_t := (X_t^1,\ldots,X_t^d)$, which satisfies the stochastic differential (17) driven by at most two noises $dW_t^1,\ldots,dW_t^m$:

$$dX_t^i \;=\; a^i(t,\boldsymbol{X}_t)dt+\sum_{j=1}^{m} b^{i,j}(t,\boldsymbol{X}_t)dW_t^j, \tag{17}$$

where for all $i=1,\ldots,d$, and $j=1,\ldots,m$, the drift vector $(a_t^i)_{t\in[0,T]}$ and the diffusion matrix $(b_t^{i,j})_{t\in[0,T]}$ are $\mathcal{F}_t$ adapted and satisfy $\int_0^T a_s^i ds<\infty$ and $\int_0^T (b_s^{i,j})^2 ds<\infty$ a.s.

For any partition $0=t_0<t_1<\cdots<t_N=T$ of the time interval $[0,T]$ with step sizes $\Delta t_n = t_{n+1}-t_n$ and maximum step-size $\Delta=\max_n \Delta t_n$, let Y_n^Δ be a numerical approximation of the exact solution X_{t_n} at a time point t_n. We have to distinguish between the strong and the weak convergence of X_{t_n}, see [7, 8]:

Definition 3. *We said that the Y_n is a strong approximation of order $\gamma=0.5,1,1.5,\ldots$ if it exists $K_{p,T}>0$ such that*

$$E_s^\gamma(Y_n^\Delta) := \Big(E|Y_{N_T}^\gamma - X_T|^p\Big)^{\frac{1}{p}} \le K_{p,T}\Delta^\gamma \quad \textit{with} \quad \lim_{N_T\to\infty} E_s^\gamma(Y_n^\Delta)=0, \tag{18}$$

and we said that Y_n is a weak approximation of order $\beta=1,2,3,\ldots$ if it exists $K_{g,T}>0$ such that

$$E_w^\beta(Y_n^\Delta) := \Big|Eg\Big(Y_{N_T}^\beta\Big) - Eg(X_T)\Big| \le K_{g,T}\Delta^\beta \quad \textit{with} \quad \lim_{N_T\to\infty} E_w^\beta(Y_n^\Delta)=0, \tag{19}$$

where g any polynomial function and p is in general one or two. Moreover, we have to note that the numerical approximation above are given in L^2.

In the following, we set clear the Itô-Taylor family scheme. We consider a regular function $f:\mathbb{R}^d\to\mathbb{R}$ and suppose that the assumptions of the existence of the numerical solution given in [7] are satisfied. Thus, the strong Itô-Taylor scheme of order $\gamma=0.5,\ 1,\ 1.5,\ 2,\ldots$ is given by:

$$\begin{aligned} Y_0 &= \xi_0, \\ Y_{n+1} &= \sum_{\alpha\in\mathcal{A}_\gamma} I_\alpha[f_\alpha(t_n,Y_n)]_{t_n,t_{n+1}} = Y_n + \sum_{\alpha\in\mathcal{A}_\gamma\setminus\{v\}} I_\alpha[f_\alpha(t_n,Y_n)]_{t_n,t_{n+1}}, \end{aligned} \tag{20}$$

where the multiple Itô-Integrals are given by definition 2, and $\mathcal{A}_\gamma$ is given by

$$\mathcal{A}_\gamma \;=\; \{\alpha\in\mathcal{M}_m|\ \ell(\alpha)+n(\alpha)=2\gamma \text{ or } \ell(\alpha)=n(\alpha)=\gamma+0.5\}. \tag{21}$$

For the weak approximation, we change the the index set $\mathcal{A}_\gamma$ by $\mathcal{A}_\beta$ such that

$$\mathcal{A}_\beta \;=\; \{\alpha\in\mathcal{M}_m|\ \ell(\alpha)\le\beta\}. \tag{22}$$

Thus, the scheme (20) could be written as:

$$
\begin{aligned}
Y_0 &= \xi_0, \\
Y_{n+1} &= Y_n + I_{(0)}[a(t,Y_n)]_{\Delta t_n} + \sum_{j_1\in F_m^1} I_{(j_1)}[b^{j_1}(t,Y_n)]_{\Delta t_n} && (23)\\
&+ \sum_{(j_1,j_2)\in F_m^2} I_{(j_1,j_2)}[L^{j_1}b^{j_2}(t,Y_n)]_{\Delta t_n} && (24)\\
&+ \sum_{(j_1,0)\in F_m^1\times\{0\}} I_{(j_1,0)}[L^{j_1}a(t,Y_n)]_{\Delta t_n} \\
&+ \sum_{(0,j_2)\in\{0\}\times F_m^1} I_{(0,j_2)}[L^{0}b^{j_2}(t,Y_n)]_{\Delta t_n} \\
&+ I_{(0,0)}[L^{0}a(t,Y_n)]_{\Delta t_n} \\
&+ \sum_{(j_1,j_2,j_3)\in F_m^3} I_{(j_1,j_2,j_3)}[L^{j_1}L^{j_2}b^{j_3}(t,Y_n)]_{\Delta t_n} && (25)\\
&+ \sum_{(j_1,j_2,0)\in F_m^2\times\{0\}} I_{(j_1,j_2,0)}[L^{j_1}L^{j_2}a(t,Y_n)]_{\Delta t_n} \\
&+ \sum_{(j_1,0,j_2)\in F_m\times\{0\}\times F_m} I_{(j_1,0,j_3)}[L^{j_1}L^{0}b^{j_3}(t,Y_n)]_{\Delta t_n} \\
&+ \sum_{(0,j_2,j_3)\in\{0\}\times F_m^2} I_{(0,j_2,j_3)}[L^{0}L^{j_2}b^{j_3}(t,Y_n)]_{\Delta t_n} \\
&+ \sum_{(j_1,j_2,j_3,j_4)\in F_m^4} I_{(j_1,j_2,j_3,j_4)}[L^{j_1}L^{j_2}L^{j_3}b^{j_4}(t,Y_n)]_{\Delta t_n}, && (26)
\end{aligned}
$$

where the Euler Maruyama scheme is represented by (23), the Milstein (or Taylor order one) is (23)-(24), Taylor scheme of order 1.5 is represented by (23)-(25) and the Taylor scheme of order 2.0 is represented by the (23)-(26), for $i = 1,\dots,d$ and $j = 1,\dots,m$ the differential operators L^j for $j = 0,1,\dots,m$ are given by

$$
\begin{aligned}
L^0 &= \frac{\partial}{\partial t} + \sum_{k=1}^{d} a_t^k \frac{\partial}{\partial x^k} + \frac{1}{2}\sum_{k,i=1}^{d}\sum_{j=1}^{m} b^{i,j}b^{k,j}\frac{\partial^2}{\partial x^i \partial x^k}, && (27)\\
L^j &= \sum_{i=1}^{d} b^{i,j}\frac{\partial}{\partial x^i}. && (28)
\end{aligned}
$$

The Itô-Taylor schemes (23)-(26) correspond to the following multi-index sets: For $\gamma = 0$ the multi-index α has a no-length, therefore the main set is $\mathcal{A}_{0.0} = \{v\}$. The set $\mathcal{A}_{0.0}$ represents the initial guess of the numerical scheme. If $\gamma = 0.5$, then the length of the multi-index is at most one. Hence, we obtain

$$\mathcal{A}_{0.5} = \mathcal{A}_{0.0} \cup \{0\} \cup F_m^1, \tag{29}$$

which leads to the Euler-Maruyama scheme. If $\gamma = 1$, then the index set $\mathcal{A}_{1.0}$ corresponds to the first order Itô-Taylor scheme (called also Milstein scheme)

$$\mathcal{A}_{1.0} = \mathcal{A}_{0.5} \cup F_m^2 = \mathcal{A}_{0.0} \cup \{0\} \cup F_m^1 \cup F_m^2. \tag{30}$$

If $\gamma = 1.5$, then index-set $\mathcal{A}_{1.5}$ is given by

$$\mathcal{A}_{1.5} = \mathcal{A}_{1.0} \cup \{(0,0)\} \cup \Big(\{0\} \times F_m^1\Big) \cup \Big(F_m^1 \times \{0\}\Big) \cup F_m^3. \tag{31}$$

If $\gamma = 2.0$ the index-set $\mathcal{A}_{2.0}$ is given by

$$\mathcal{A}_{2.0} = \mathcal{A}_{1.5} \cup \Big(\{0\} \times F_m^2\Big) \cup \Big(F_m^2 \times \{0\}\Big) \cup \Big(F_m^1 \times \{0\} \times F_m^1\Big) \cup F_m^4. \tag{32}$$

4 Time-space integration of SPDS on overlapping interface

Consider a constant time step Δt of the time interval $\mathbb{T} = [0, T]$ and constant spatial steps $\Delta x = x_{i+1} - x_i = \Delta y = y_{j+1} - y_j$, for $i = 1, \ldots, N$ and $j = 1, \ldots, M$ Thus, the FTCS approximation of the solution of (1) is

$$\begin{aligned} dU_{i,j}^1(t) &= \Big[(-2\alpha)U_{i,j}^1(t) + \frac{\alpha}{2}\beta^- U_{i-1,j}^1(t) + \frac{\alpha}{2}\beta^+ U_{i+1,j}^1(t) \\ &\quad + \frac{\alpha}{2}\beta^- U_{i,j-1}^1(t) + \frac{\alpha}{2}\beta^+ U_{i,j+1}^1\Big]dt + \sigma^1\eta^1(t, \mathbf{x}_{i,j}, \omega)dt \\ dU_{i,j}^2(t) &= \Big[(-2\alpha)U_{i,j}^2 + \frac{\alpha}{2}\beta^- U_{i-1,j}^2(t) + \frac{\alpha}{2}\beta^+ U_{i+1,j}^2(t) \\ &\quad + \frac{\alpha}{2}\beta^- U_{i,j-1}^2(t) + \frac{\alpha}{2}\beta^+ U_{i,j+1}^2(t)\Big]dt + \sigma^2\eta^2(t, \mathbf{x}_{i,j}, \omega)dt \end{aligned} \tag{33}$$

where $U_{i,j}^s \approx \boldsymbol{U}^s(\mathbf{x}_{i,j}, t) = \boldsymbol{U}^s((x_i, y_j), t)$ represents the numerical approximation of the exact solution $\boldsymbol{U}^s$ at the space-time point $((x_i, y_j), t) \in \boldsymbol{D} \times \mathbb{T}$. The coefficients α, β^+ and β^- are given as

$$\frac{\alpha}{\Delta t} = \frac{2d}{(\Delta x)^2}, \qquad \beta^- = 1 - \frac{a}{2d}\Delta x, \quad \text{and} \quad \beta^+ = 1 + \frac{a}{2d}\Delta x. \tag{34}$$

The system (33) can be transformed into a multidimensional stochastic differential system of the form, see similar works [24]

$$\begin{cases} d\boldsymbol{U}^1(t) &= \mathbf{K}^1(t, \boldsymbol{U}^1(t))dt + \mathbf{G}^1(t)d\mathbf{W}^1(t), \quad \text{on} \quad \boldsymbol{D}_1, \\ d\boldsymbol{U}^2(t) &= \mathbf{K}^2(t, \boldsymbol{U}^2(t))dt + \mathbf{G}^2(t)d\mathbf{W}^2(t), \quad \text{on} \quad \boldsymbol{D}_2, \end{cases} \tag{35}$$

where the white noise stochastic processes $\eta^s(t, \mathbf{x}, \cdot)$ are supposed to be uncorrelated in time and in space for all $s = 1, 2$, it yields

$$d t\eta^s(t, \mathbf{x}, \omega) := \begin{cases} dW^s(t, \mathbf{x}, \omega) & \text{if} \quad \mathbf{x} \in D_s \subseteq D, \\ 0 & \text{Otherwise,} \end{cases}$$

Moreover, the white noise processes dW^s is Hilbert-space valued random variable satisfying:

$$dW^s(t, \mathbf{x}, \cdot)dW^s(t, \mathbf{y}, \cdot) = 2f(\mathbf{x} - \mathbf{y})dt,$$

where $s = 1, 2$, $\mathbf{x}, \mathbf{y} \in D_s$ and f is a smooth function. It should be stressed that, in the general case, it is not required that the noises η^s to be independent and identically distributed. Furthermore, the white noise or Brownian motion can be considered as a truncated approximation of infinite dimensional Wiener process [4].

Our main interest is solving the system (35) numerically by taking in consideration the overlapping interface $\Gamma_{1,2}$. Therefore, we define the evolution of $\boldsymbol{U}^1$ and $\boldsymbol{U}^2$ as combined solution $\boldsymbol{U}^3$, as suggested by the reactions 4. This resulting solution could be interpreted as the outcome of chemical or biological reactions. Thus, we assume that there exist $\alpha_t \in [0, 1]$ such that

$$\boldsymbol{U}_t^3 \;=\; \alpha_t \boldsymbol{U}_t^1 + (1 - \alpha_t)\boldsymbol{U}_t^2 \quad \text{on} \quad \Gamma_{1,2}. \tag{36}$$

Hence, the stochastic system could be written as

$$\begin{cases} d\boldsymbol{U}^1(t) &= \mathbf{K}^1(t, \boldsymbol{U}^1(t))dt + \mathbf{G}^1(t)d\mathbf{W}^1(t) & \text{on} \quad \boldsymbol{D}_1 \setminus \Gamma_{1,2}, \\ d\boldsymbol{U}^2(t) &= \mathbf{K}^2(t, \boldsymbol{U}^2(t))dt + \mathbf{G}^2(t)d\mathbf{W}^2(t) & \text{on} \quad \boldsymbol{D}_2 \setminus \Gamma_{1,2}, \\ d\boldsymbol{U}^3(t) &= \mathbf{K}^3(t, \boldsymbol{U}^3(t))dt + \mathbf{G}^1(t)d\mathbf{W}^1(t) + \mathbf{G}^2(t)d\mathbf{W}^2(t) & \text{on} \quad \Gamma_{1,2}. \end{cases} \tag{37}$$

where $\mathbf{K}^i$, $\mathbf{G}^i$ and $\mathbf{W}^i$ for $i = 1, 2, 3$ are matrix resulting from discretizating system using the deterministic method of lines, se for more details [24, 34]. Furthermore, the system (37) should be solved for $\boldsymbol{U}^1$ on $(\boldsymbol{D}_1 \setminus \Gamma_{1,2})$, $\boldsymbol{U}^2$ on $(\boldsymbol{D}_2 \setminus \Gamma_{1,2})$ and for $\boldsymbol{U}^3$ on $\Gamma_{1,2}$ considering the combination (36). However, the solution on the non overlapping interface $\partial\Gamma_{1,2} = \Gamma_d \cup \Gamma_u$, satisfies, the following continuity condition

$$\begin{cases} \boldsymbol{U}^1 &= \boldsymbol{U}^3 \quad \text{for} \quad (\mathbf{x}, t) \in \Gamma_d \times \mathbb{T}, \\ \boldsymbol{U}^2 &= \boldsymbol{U}^3 \quad \text{for} \quad (\mathbf{x}, t) \in \Gamma_u \times \mathbb{T}. \end{cases} \tag{38}$$

where the interface (38) will be interpolated using the Barycentric interpolation method given by (13). It is important to note that integrating the iterated stochastic integrals I_α, for a multi-index α does not need any approximation on $\boldsymbol{D}_1 \setminus \Gamma_{1,2}$ and $\boldsymbol{D}_2 \setminus \Gamma_{1,2}$ since the random excitation desponds on one noise only, see the explicit construction in [34]. While in on the common overlapped interface the double stochastic integral $I_{(j_1,j_2)}$, for $j_1 \neq j_2$ needs to be approximated using classical methods, see for instance [32].

5 Numerical experiments

The main goal of our numerical tests, is analyzing the numerical behavior of the solution on domains with an overlapped interface. We simulate the SPDS (1) together with (5) on D showed in Fig. 2. We restrict ourself to the problem in dimension two and for the error measurement, we use the L^2 grid norm:

$$\left\| \boldsymbol{U} - U^{DD} \right\|_2 \;=\; \Delta x \left(\sum_{i=1}^{N_x} \sum_{j=1}^{N_x} |U_{i,j} - U_{i,j}^{DD}|^2 \right)^{1/2}. \tag{39}$$

First, we consider the following cut functions:

$$f_d(x) \;=\; -0.505 - 0.15e^{-15(x-0.5)^2}; \quad \text{and} \quad f_u(x) = 0.5 + 0.15e^{-15(x-0.5)^2}. \tag{40}$$

Thus, the computational subdomains are then given by:

(i) $\boldsymbol{D} := \left\{\mathbf{x} = (x,y) \in C(\mathbf{x}_0, r) \middle| \; (x-1/2)^2 + (y-1/2)^2 \leq 1/4\right\} = D(\mathbf{x}_0, r).$

(ii) $\boldsymbol{D}_1 := \left\{\mathbf{x} = (x,y) \in D(\mathbf{x}_0, r) \middle| \; x \leq f_u(x)\right\}.$

(iii) $\boldsymbol{D}_2 := \left\{\mathbf{x} = (x,y) \in D(\mathbf{x}_0, r) \middle| \; f_d(x) \leq x\right\}.$

(iv) $\Gamma_{1,2} := \left\{\mathbf{x} = (x,y) \in D(\mathbf{x}_0, r) \middle| \; f_d(x) \leq x \leq f_u(x)\right\},$

where $C(\mathbf{x}_0, r)$ is the circle with center $\mathbf{x}_0 = (1/2, 1/2)$ and radius $r = 1/2$ and $D(\mathbf{x}_0, r)$ is the corresponding Disc. The non-overlapping interfaces are given in the following set notation

(iii) $\Gamma_u := \left\{\mathbf{x} = (x,y) \in \Gamma_{1,2} \middle| \; y = f_u(x)\right\}.$

(iv) $\Gamma_d := \left\{\mathbf{x} = (x,y) \in \Gamma_{1,2} \middle| \; y = f_d(x)\right\}.$

where the boundary of the interface is given by $\partial\Gamma_{1,2} = \Gamma_d \cup \Gamma_u$.

We simulate our result on the following computational domains Under different initial

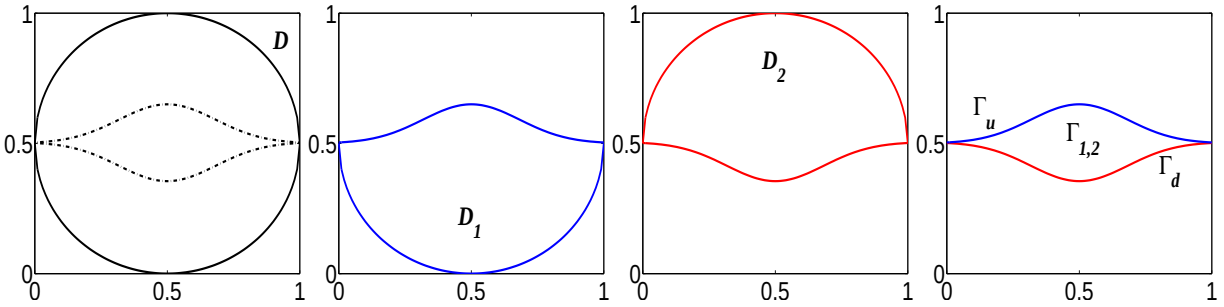

(a) Domain D (b) Subdomain D_1 (c) Subdomain D_2 (d) $\Gamma_{1,2} = D_1 \cap D_2$

Figure 2: Computational subdomains.

solutions and different choice of the advection and diffusion coefficients, we solve the non-overlapping advection diffusion system (41), which is equivalent to the original problem (1):

$$\begin{cases} \boldsymbol{U}_t^1 &= d\Delta\boldsymbol{U}^1 + a\nabla\boldsymbol{U}^1 \quad \text{for} \quad (\mathbf{x},t) \in \boldsymbol{D}_1 \times \mathbb{T}, \\ \boldsymbol{U}_t^2 &= d\Delta\boldsymbol{U}^2 + a\nabla\boldsymbol{U}^2 \quad \text{for} \quad (\mathbf{x},t) \in \boldsymbol{D}_2 \times \mathbb{T}, \\ \boldsymbol{U}_t^3 &= d\Delta\boldsymbol{U}^3 + a\nabla\boldsymbol{U}^3 \quad \text{for} \quad (\mathbf{x},t) \in \Gamma_{1,2} \times \mathbb{T}, \\ \boldsymbol{U}^1 &= \boldsymbol{U}^3 \quad \text{for} \quad (\mathbf{x},t) \in \Gamma_d \times \mathbb{T}, \\ \boldsymbol{U}^2 &= \boldsymbol{U}^3 \quad \text{for} \quad (\mathbf{x},t) \in \Gamma_u \times \mathbb{T}. \end{cases} \tag{41}$$

For all our simulation, we adjust the time-space stability condition using the Courant Friedrichs Lewy condition $\Delta t = 0.95(\Delta t)_{CFL}$, where $(\Delta t)_{CFL} = \dfrac{(\Delta x)^2}{4\mathbf{d}}$.

5.1 TEST 1: Decoupling vs coupling of local solutions

In this test, we perform a geometrical accuracy test. We solve the problem (42) using the coefficients $d_k = 0.25$ and $a_k = 0.2$, for $k = 1, 2, 3$. We examine the decoupling behavior of the three solutions by solving $\boldsymbol{U}^1$ on $\boldsymbol{D}_1 \setminus \Gamma_{1,2}$, $\boldsymbol{U}^2$ on $\boldsymbol{D}_2 \setminus \Gamma_{1,2}$, and $\boldsymbol{U}^3$ on $\Gamma_{1,2}$:

$$(P_1): \begin{cases} \boldsymbol{U}^1_t &= d_1 \Delta \boldsymbol{U}^1 + a_1 \nabla \boldsymbol{U}^1 \quad \text{for} \quad (\mathbf{x}, t) \in \boldsymbol{D}_1 \times \mathbb{T}, \\ \boldsymbol{U}^2_t &= d_2 \Delta \boldsymbol{U}^2 + a_2 \nabla \boldsymbol{U}^2 \quad \text{for} \quad (\mathbf{x}, t) \in \boldsymbol{D}_2 \times \mathbb{T}, \\ \boldsymbol{U}^3_t &= d_3 \Delta \boldsymbol{U}^3 + a_3 \nabla \boldsymbol{U}^3 \quad \text{for} \quad (\mathbf{x}, t) \in \Gamma_{1,2} \times \mathbb{T}. \end{cases} \tag{42}$$

We compare the geometrical behavior of the non-interpolated interface solution (ie $\mathbf{w} \equiv 0$)

$$\begin{aligned} \boldsymbol{U}^1 &= \boldsymbol{U}^3 = 0 \quad \text{for} \quad (\mathbf{x}, t) \in \Gamma_d \times \mathbb{T}, \\ \boldsymbol{U}^2 &= \boldsymbol{U}^3 = 0 \quad \text{for} \quad (\mathbf{x}, t) \in \Gamma_u \times \mathbb{T}, \end{aligned} \tag{43}$$

with the interpolated one ($\mathbf{w} \neq 0$)

$$\begin{aligned} \boldsymbol{U}^1 &= \boldsymbol{U}^3 = \mathbf{w}^{1,3} \quad \text{for} \quad (\mathbf{x}, t) \in \Gamma_d \times \mathbb{T}, \\ \boldsymbol{U}^2 &= \boldsymbol{U}^3 = \mathbf{w}^{2,3} \quad \text{for} \quad (\mathbf{x}, t) \in \Gamma_u \times \mathbb{T}. \end{aligned} \tag{44}$$

The initial solutions are the following normal-like concentrations:

$$\begin{cases} \boldsymbol{U}^1(\mathbf{x}, 0) = \exp\Big(-0.15\Big(\dfrac{(x-0.5)^2 + (y-0.2)^2}{2 \cdot 10^{-4}}\Big)\Big) \quad \text{on} \quad \boldsymbol{D}_1 \setminus \Gamma_{1,2}, \\ \boldsymbol{U}^2(\mathbf{x}, 0) = \exp\Big(-0.15\Big(\dfrac{(x-0.5)^2 + (y-0.5)^2}{2 \cdot 10^{-4}}\Big)\Big) \quad \text{on} \quad \boldsymbol{D}_2 \setminus \Gamma_{1,2}, \\ \boldsymbol{U}^3(\mathbf{x}, 0) = \exp\Big(-0.15\Big(\dfrac{(x-0.5)^2 + (y-0.8)^2}{2 \cdot 10^{-4}}\Big)\Big) \quad \text{on} \quad \Gamma_{1,2}, \end{cases} \tag{45}$$

The Dirichlet boundary conditions for the three solutions are:

$$\begin{cases} \boldsymbol{U}^1(\mathbf{x}, t) &= 0 \quad \text{for all} \quad (\mathbf{x}, t) \in \partial(\boldsymbol{D}_1 \setminus \Gamma_{1,2}) \times [0, T], \\ \boldsymbol{U}^2(\mathbf{x}, t) &= 0 \quad \text{for all} \quad (\mathbf{x}, t) \in \partial(\boldsymbol{D}_2 \setminus \Gamma_{1,2}) \times [0, T], \\ \boldsymbol{U}^3(\mathbf{x}, t) &= 0 \quad \text{for all} \quad (\mathbf{x}, t) \in \partial(\Gamma_{1,2}) \times [0, T], \end{cases} \tag{46}$$

In the first row of Figure 3, we present the decoupled solutions $\boldsymbol{U}^1$, $\boldsymbol{U}^2$ and $\boldsymbol{U}^2$ defined by (42). We show the solutions at different time steps, namely at $t = 0$, $t = 100\Delta t$, $t = 200\Delta t$ and $t = 500\Delta t$. The plotted contours are fully separated since the inside interface is a zero-flux boundary. This confirms on the one hand the control of the interface and on the other hand the possibility to simulate different problems on the non-overlapping subdomains $\boldsymbol{D}_1 \setminus \Gamma_{1,2}$, $\boldsymbol{D}_2 \setminus \Gamma_{1,2}$ and $\Gamma_{1,2}$, respectively. In the second row of Figure 3, we show the solution of the problem (42) by interpolating the interface solution (44) using the BIM algorithm.

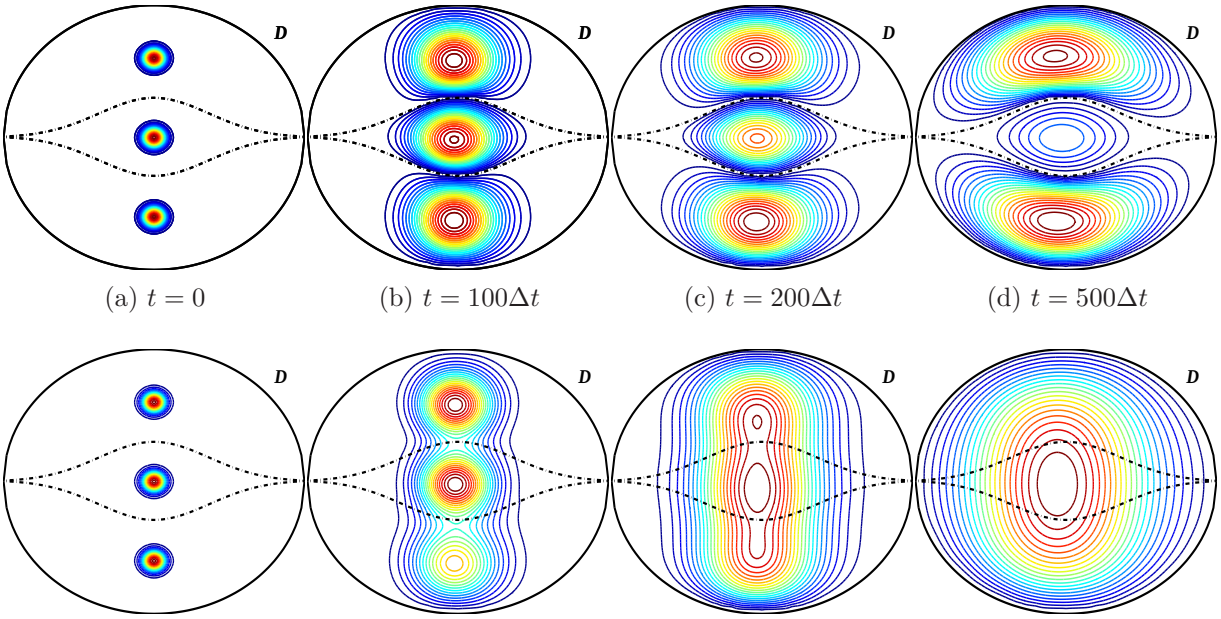

(a) $t = 0$ (b) $t = 100\Delta t$ (c) $t = 200\Delta t$ (d) $t = 500\Delta t$

(e) $t = 0$ (f) $t = 100\Delta t$ (g) $t = 200\Delta t$ (h) $t = 500\Delta t$

Figure 3: Decoupling vs coupling of local solutions on $\boldsymbol{D}_1 \setminus \Gamma_{1,2}$, $\boldsymbol{D}_2 \setminus \Gamma_{1,2}$ and on $\Gamma_{1,2}$.

5.2 TEST 2: Interface smoothing

The main goal of this test is to observe the behavior of the interface solution and the solutions on the neighborhood the inside interfaces. In this experiment, we solve the problem (42) by interpolating the interface solution. We approximate $\boldsymbol{U}^1$ on $\boldsymbol{D}_1 \setminus \Gamma_{1,2}$, $\boldsymbol{U}^2$ on $\boldsymbol{D}_2 \setminus \Gamma_{1,2}$, and $\boldsymbol{U}^3$ on $\Gamma_{1,2}$ such that $\boldsymbol{U}^3 := \boldsymbol{U}^1 + \boldsymbol{U}^2$. The initial solution is generated using a uniform random variable with values in $(0, 10^{-4})$.

For different diffusion and advection coefficients $d_1 = 0.25$, $a_1 = 0.2$, $d_2 = 0.2$, $a_2 = 0.25$ and $d_3 = (d_1 + d_2)/2$, $a_3 = (a_1 + a_2)/2$, we present in Figure (4) the evolution of the initial solution at three time steps $t = \Delta t$, $t = 10\Delta t$ and at $t = 100\Delta t$. In Figure (5), we show the cross section at $x = 0.5$ for the same solutions above. The expected result is getting a smooth surface of the two dimensional function, which is the case. For equal coefficients, we refer to the first case. The second row of Fig. 4 shows a perfect coupling of the solutions. These solution are geometrically smooth enough to be at least two times continuous and differentiable. Moreover, it should be stressed that even the starting initial solution is fully irregular and the steady-state solution is a differentiable surface. Moreover, we pay attention of the reader that the geometrical asymptotic behavior of the limit solution is in general independent from the choice of the initial solutions.

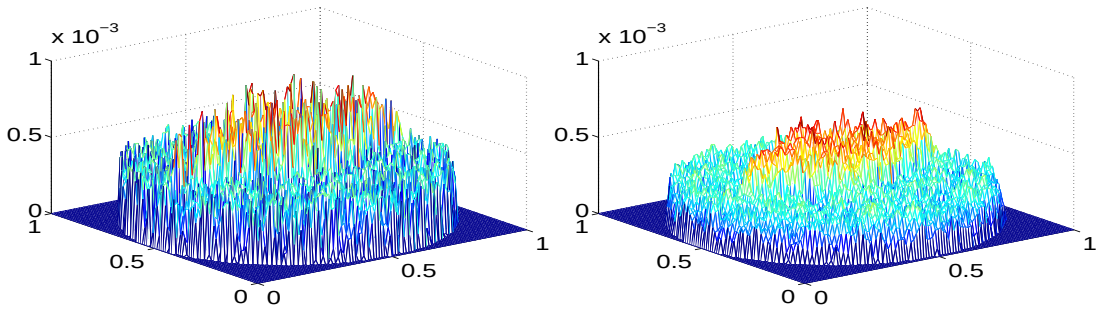

(a) $t = 0$ (b) $t = 1\Delta t$

(c) $t = 10\Delta t$ (d) $t = 100\Delta t$

Figure 4: Interface smoothing: Sol. $\boldsymbol{U}^1$ on $\boldsymbol{D}_1 \setminus \Gamma_{1,2}$, $\boldsymbol{U}^2$ on $\boldsymbol{D}_2 \setminus \Gamma_{1,2}$ and $\boldsymbol{U}^3$ on $\Gamma_{1,2}$.

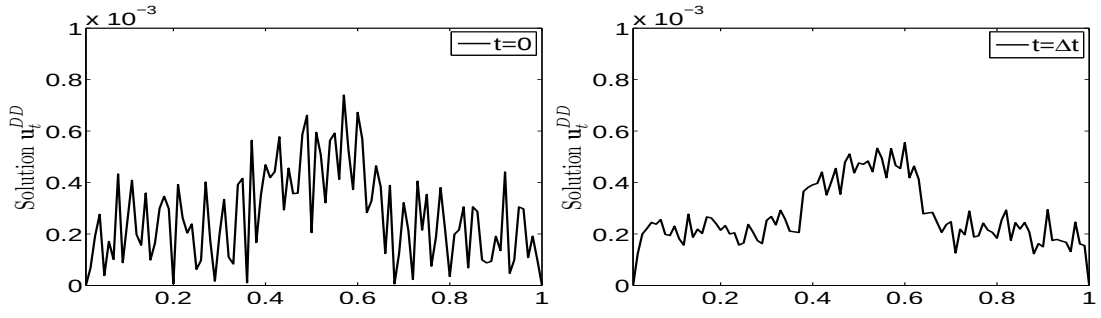

(a) $t = 0$ (b) $t = 1\Delta t$

(c) $t = 10\Delta t$ (d) $t = 100\Delta t$

Figure 5: Cross section solutions at $x = 0.5$.

5.3 TEST 3: Convergence accuracy

In this test, we numerically accurate the combined method FTCS-BIM for solving evolutionary IBV problems. We compute the computational convergence rate CCO by solving $\boldsymbol{U}^1$ on $\boldsymbol{D}_1 \setminus \Gamma_{1,2}$, $\boldsymbol{U}^2$ on $\boldsymbol{D}_2 \setminus \Gamma_{1,2}$, and $\boldsymbol{U}^3 = (\boldsymbol{U}^1 + \boldsymbol{U}^2)/2$ on $\Gamma_{1,2}$:

$$(P3): \left\{ \begin{array}{lll} \boldsymbol{U}_t^1 & = d_1 \Delta \boldsymbol{U}^1 + a_1 \nabla \boldsymbol{U}^1 & \text{for} \quad (\mathbf{x}, t) \in \boldsymbol{D}_1 \times \mathbb{T}, \\ \boldsymbol{U}_t^2 & = d_2 \Delta \boldsymbol{U}^2 + a_2 \nabla \boldsymbol{U}^2 & \text{for} \quad (\mathbf{x}, t) \in \boldsymbol{D}_2 \times \mathbb{T}, \\ \boldsymbol{U}_t^3 & = d_3 \Delta \boldsymbol{U}^3 + a_3 \nabla \boldsymbol{U}^3 & \text{for} \quad (\mathbf{x}, t) \in \Gamma_{1,2} \times \mathbb{T}. \end{array} \right. \tag{47}$$

We compare the solution of (47) by interpolating the interface solution with the solution of

$$\boldsymbol{U}_t \quad = d_\Sigma \Delta \boldsymbol{U} + a_\Sigma \nabla \boldsymbol{U} \quad \text{for} \quad (\mathbf{x}, t) \in \boldsymbol{D} \times \mathbb{T}, \tag{48}$$

where $\boldsymbol{U}^k$ is the projection of $\boldsymbol{U}$ on Σ for $k = 1, 2, 3$ and Σ represents the subdomains $\boldsymbol{D}_1 \setminus \Gamma_{1,2}$, $\boldsymbol{D}_2 \setminus \Gamma_{1,2}$, and $\Gamma_{1,2}$. We set

$$d_{\boldsymbol{D}_1 \setminus \Gamma_{1,2}} = d_1; \quad d_{\boldsymbol{D}_2 \setminus \Gamma_{1,2}} = d_2; \quad d_{\Gamma_{1,2}} = (d_1 + d_2)/2, \tag{49}$$

and

$$a_{\boldsymbol{D}_1 \setminus \Gamma_{1,2}} = d_1; \quad a_{\boldsymbol{D}_2 \setminus \Gamma_{1,2}} = a_2; \quad a_{\Gamma_{1,2} \setminus \partial\Gamma_{1,2}} = (a_1 + a_2)/2, \tag{50}$$

Under the Dirichlet boundary conditions and the following initial solution

$$\boldsymbol{U}(\mathbf{x}, 0) = \exp(-30((x - 0.5)^2 + (y - 0.5)^2)). \tag{51}$$

we distinguish two cases:

A: Using equal coefficients: $d_1 = d_2 = 0.25$ and $a_1 = a_2 = 0.2$.

B: Using different coefficients $d_1 = 0.25$, $a_1 = 0.2$ and $d_2 = 0.2$, $a_2 = 0.25$.

We assume moreover the following interface equality

$$\boldsymbol{U}^1 \mid_{\Gamma_d} = \boldsymbol{U}^3 \mid_{\Gamma_d} \quad \text{and} \quad \boldsymbol{U}^2 \mid_{\Gamma_u} = \boldsymbol{U}^3 \mid_{\Gamma_u} . \tag{52}$$

The interface solution on $\partial\Gamma_{1,2}$ is defined by

$$\mathbf{w}^{1,3}(\mathbf{x}, t) \quad := \quad \boldsymbol{U}^1(\mathbf{x}, t) = \boldsymbol{U}^3(\mathbf{x}, t) \quad \text{on} \quad (\mathbf{x}, t) \in \Gamma_u \times [0, T], \tag{53}$$

$$\mathbf{w}^{2,3}(\mathbf{x}, t) \quad := \quad \boldsymbol{U}^2(\mathbf{x}, t) = \boldsymbol{U}^3(\mathbf{x}, t) \quad \text{on} \quad (\mathbf{x}, t) \in \Gamma_d \times [0, T]. \tag{54}$$

As can be remarked in Table 1., the method FTCS-BIM assure the second order in space. The first order CCO is guaranteed, since the used temporal step is chosen using the CFL stability condition: $\Delta t = 0.95(\Delta t)_{CFL}$, where $(\Delta t)_{CFL} = (\Delta x)^2/4max(d_k, a_k)$.

Table 1: Spatial L^2-errors for the cases A and B.

	case A		case B	
N_x	L^2-error	CCO	L^2-error	CCO
25	2.085266E-3	–	3.072218E-3	–
50	1.977757E-4	–	5.322484E-4	–
100	2.970599E-5	3.0666	1.243835E-4	2.3132
200	4.084231E-6	2.7988	3.014155E-5	2.0711
400	7.294578E-7	2.6738	7.511688E-6	2.0247

5.4 TEST 4: Solving overlapping SPDEs

In this test we solve the stochastic partial differential system

$$(P_4)\ \begin{cases} \boldsymbol{U}_t^1 = d_1\Delta\boldsymbol{U}^1 - a_1\nabla\boldsymbol{U}^1 + \sigma^1\eta^1 \quad \text{on} \quad \boldsymbol{D}_1 \setminus \Gamma_{1,2}, \\ \boldsymbol{U}_t^2 = d_2\Delta\boldsymbol{U}^2 - a_2\nabla\boldsymbol{U}^2 + \sigma^2\eta^2 \quad \text{on} \quad \boldsymbol{D}_2 \setminus \Gamma_{1,2}, \\ \boldsymbol{U}_t^3 = d_3\Delta\boldsymbol{U}^3 - a_3\nabla\boldsymbol{U}^3 + \sigma^1\eta^1 + \sigma^2\eta^2 \quad \text{on} \quad \Gamma_{1,2}, \end{cases} \tag{55}$$

We numerically approximate the solution of the system (6) using the first order Milstein scheme. We generate a initial solution using a uniform distributed random variable. Thereafter, we approximate the numerical solutions $\boldsymbol{U}^1\ |_{\boldsymbol{D}_1\setminus\Gamma_{1,2}}$, $\boldsymbol{U}^2\ |_{\boldsymbol{D}_2\setminus\Gamma_{1,2}}$, and $(\alpha_t\boldsymbol{U}^1 + (1-\alpha_t)\boldsymbol{U}^2)\ |_{\Gamma_{1,2}}$, for $\alpha_t \sim UR(0,1)$. Similarly to the third test, we distinguish two cases:

A: Using equal coefficients: $d_1 = d_2 = 0.25$ and $a_1 = a_2 = 0.2$.

B: Using different coefficients $d_1 = 0.25$, $a_1 = 0.2$ and $d_2 = 0.2$, $a_2 = 0.25$.

We assume moreover the following interface equality and set

$$d_{\boldsymbol{D}_1\setminus\Gamma_{1,2}} = d_1; \quad d_{\boldsymbol{D}_2\setminus\Gamma_{1,2}} = d_2; \quad d_{\Gamma_{1,2}} = (d_1+d_2)/2, \tag{56}$$

and

$$a_{\boldsymbol{D}_1\setminus\Gamma_{1,2}} = d_1; \quad a_{\boldsymbol{D}_2\setminus\Gamma_{1,2}} = a_2; \quad a_{\Gamma_{1,2}\setminus\partial\Gamma_{1,2}} = (a_1+a_2)/2, \tag{57}$$

In Figure (6), we present in the first row the evolution of the solution at three time steps od the case A: At $t = 100\Delta t$, $t = 200\Delta t$ and $t = 5000\Delta t$. In the second row, we show the solution of the case B.

In Figure (7), we show a comparison overview of the initial and the Mean solution of a $M = 500$ realizations at time $t = 5000\Delta t$.

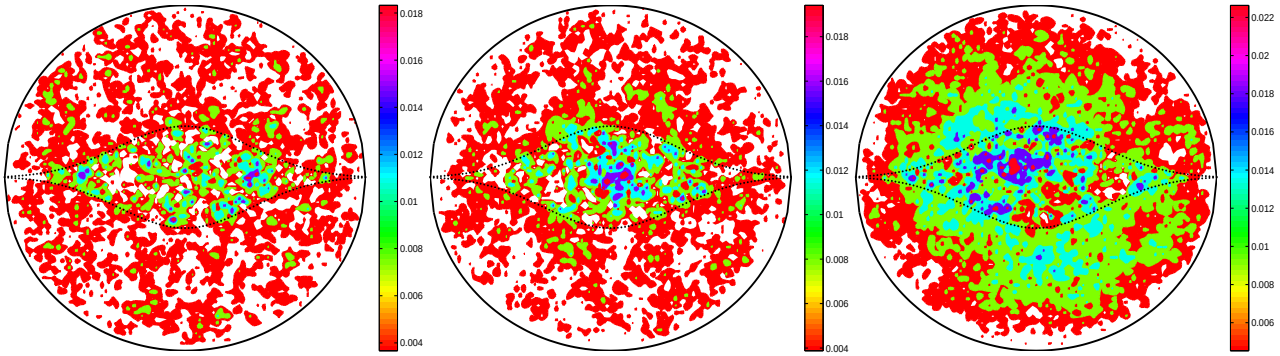

(a) A, $t = 100\Delta t$ (b) A, $t = 200\Delta t$ (c) A, $t = 5000\Delta t$

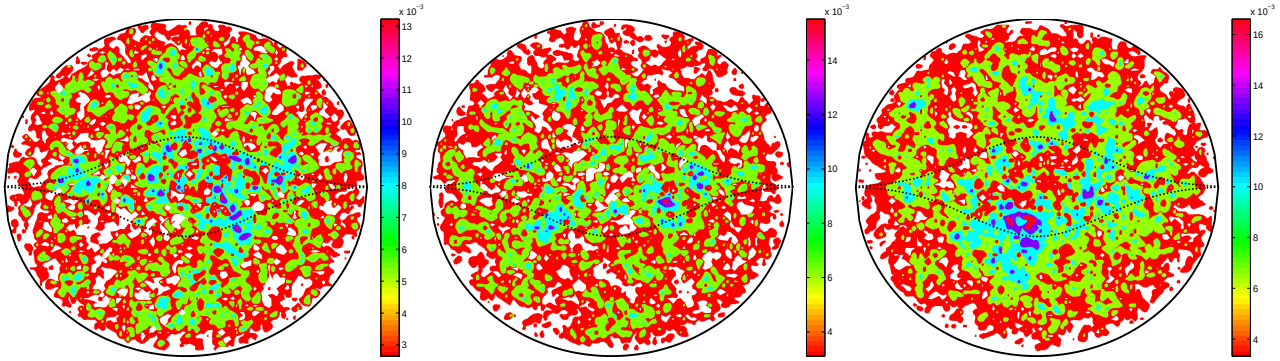

(d) B, $t = 100\Delta t$ (e) B, $t = 200\Delta t$ (f) B, $t = 5000\Delta t$

Figure 6: SPDEs solutions using equal and different advection-diffusion coefficients.

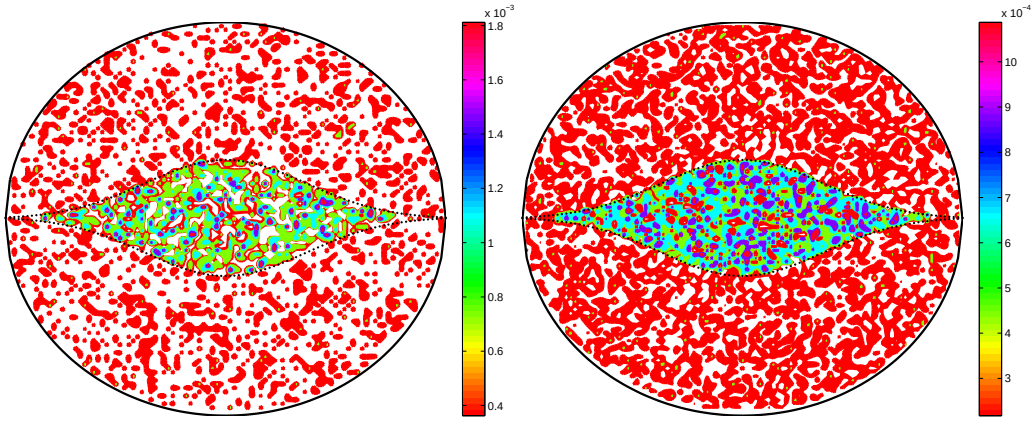

(a) $t = 0$ (b) $t = 5000\Delta t$, $M = 500$

Figure 7: Comparison of the initial and the mean solution at $t = 5000\Delta t$ of $M = 500$ realizations.

6 Concluding remarks and outlooks

We developed a new numerical method for solving stochastic partial differential systems on overlapping subdomains. We transformed the original problem into an equivalent system on non-overlapping subdomains. In addition, we numerically examined this computational approach on overlapped subdomains with nonlinear (curved) boundaries. In order to accurate our scheme, we experimented various geometrical tests using combination of different numerical schemes. Namely the domain decomposition method, the method of lines and the barycentric interpolation method. The stochastic partial differential equations are solved using the first order Itô-Taylor scheme or also the Milstein scheme. Numerically, it has to be mentioned that this method could be easily extended to interesting real applications using higher order or more suitable schemes such as Crank Nicolson, Relaxation, finite volume, finite elements and meshless. Practically, the suggested reactional region could be interpreted using more realistic data. Therefore, real life applications are our future studies. Especially the treatment of problems in medicine or oceanographic pollution problems.

Acknowledgment. This work is supported by the University of Sharjah (UOS), Research group MASEP, RGS-2018-2019, No. 1802144062-P and No. 1802144069.

REFERENCES

[1] J. P. Arachchige, G. J. Pettet, A finite volume method with linearization in time for solution of advection-reaction-diffusion systems, Appl. Math. and Comp. 231 (2014), 445-462.

[2] R. Ghanem, P.D. Spanos: Stochastic Finite Elements: A Spectral Approach. Springer-Verlag, New York, 1991.

[3] W. Gropp, B.F. Smith, Scalable, extensible, and portable numerical libraries, Proceedings of the Scalable Parallel Libraries Conference,(1993) pp. 87-93.

[4] H. Holden, B. Oksendal, J. Uboe, T. Zhang: Stochastic Partial Differential Equations: A Modeling, White Noise Functional Approach. Probability and its Applications, Birkhäuser, Basel, 1996.

[5] A. Kaya, Finite difference approximations of multidimensional unsteady convection-diffusion-reaction equations, Journal of Computational Physics 285 (2015) 331-349.

[6] A. Kaya, A finite difference scheme for multidimensional convection-diffusion-reaction equations, Computer Methods in Applied Mechanics and Engineering Volume 278, 15 (2014), 347-360

[7] Kloeden P. E., Platen E. Numerical Solution of Stochastic Differential Equations, Springer Verlag 1992.

[8] A. Jentzen, P. Kloeden, Taylor Approximations for Stochastic Partial Differential Equations, the Society for Industrial and Applied Mathematics (SIAM) 2011.

[9] P. L. Lions, On the Schwarz alternating method I., First Int. Symp. on Domain Decomposition Methods, SIAM, 1988, pp. 1–42.

[10] P. L. Lions , On the Schwarz alternating method II., Second Int. Conference on Domain Decomposition Methods, SIAM, 1989, pp. 47–70.

[11] H. W. Luo, T. Z. Huang, X. M. GU, Y. Liu, Barycentric rational collocation methods for a class of nonlinear parabolic partial differential equations, Applied mathematics letter, 68 (2017) 13-19

[12] V. Martin. A Schwarz waveform relaxation method for the viscous shallow water equations. In R. Kornhuber, R.H.W. Hoppe, J. Periaux, O. Pironneau, O.B. Widlund, and J. Xu, editors, Proceedings of the 15th International Domain Decomposition Conference. Springer, 2003.

[13] V. Martin. An optimized Schwarz waveform relaxation method for unsteady convection diffusion equation. Appl. Numer. Math., 52(4):401-428, 2005.

[14] S.H. Lui, On Schwarz alternating methods for nonlinear elliptic pdes. SIAM J. Sci. Comput. 21 (2000) 1506–1523

[15] T. Mathew, Domain Decomposition Methods for the Numerical Solution of Partial Differential Equations, Springer (2008).

[16] N. Mai-Duy, and T. Tran-Cong, An efficient domain-decomposition pseudo-spectral method for solving elliptic differential equations, Commun. Numer. Meth. Eng 24 (2008) 795-806.

[17] G.N. Milstein, M.V. Tretyakov, Layer methods for stochastic Navier–Stokes equations using simplest characteristics, Journal of Computational and Applied Mathematics 302 (2016) 1-23

[18] W.E. Schiesser, The numerical method of lines. Integration of partial differential equations, Academic Press. San Diego, CA, 1991.

[19] H. A. Schwarz, Über einen grenzübergang durch alternirendes Verfahren, Ges. Math. Abh. Bd.1 Berlin 1870, s133-143.

[20] B.F. Smith, O.B. Widlund, A domain decomposition algorithm using a hierarchical basis SIAM journal on scientific and statistical computing 11 (6),(1990), 1212-1220.

[21] B. Smith, P. Bjorstad, W. Gropp, Domain Decomposition: Parallel Multilevel Methods for Elliptic Partial Differential Equations, Cambridge University Press: Europe-North America ISBN 0-521-49589-X (2004)

[22] A. Quarteroni, A. Veneziani, P. Zunino, A Domain Decomposition Method For Advection-Diffusion Processes With Application To Blood Solutes, SIAM J. SCI. COMPUT. Vol. 23, No. 6,(2002), pp. 1959-1980.

[23] J. G. Verwer, J. M. Sanz-Serna (1984), Convergence of method of lines approximations to partial differential equations, Computing, 33(3-4), 297-313 (1984).

[24] A. Rößler , M. Seaïd , M. Zahri, Numerical simulation of stochastic replicator models in catalyzed RNA-like polymers, Mathematics and Computers in Simulation 79 (2009) 3577-3586.

[25] A. Zafarullah , Application of the Method of Lines to Parabolic Partial Differential Equations With Error Estimates, Journal of the Association for Computing Machinery, 17 (2), 294-302 (1970)

[26] R. Courant, K. Friedrichs, and H. Lewy, On the partial difference equations of mathematical physics, IBM J. Res. Develop., 11 (1967), pp. 215-234.

[27] H. W. Luo, T. Z. Huang, X. M. GU, Y. Liu, Barycentric rational collocation methods for a class of nonlinear parabolic partial differential equations, Applied mathematics letter, 68 (2017) 13-19

[28] Y. Saad and M.H. Schultz, 'GMRES: A generalized minimal residual algorithm for solving nonsymmetric linear systems', SIAM J. Sci. Stat. Comput. (1986), 7:856-869,

[29] T.J. Sun, Keying Ma, Domain decomposition procedures combined with H^1-Galerkin mixed finite element method for parabolic equation, Journal of Computational and Applied Mathematics 267 (2014), pages 33-48.

[30] A. Quarteroni, A. Veneziani, P. Zunino, A Domain Decomposition Method For Advection-Diffusion Processes With Application To Blood Solutes, SIAM J. SCI. COMPUT. Vol. 23, No. 6,(2002), pages 1959-1980.

[31] J. Xu, J. Zou, Some non-overlapping domain decomposition methods, SIAM REV., Vol. 40, No. 4, (1998) pages 857-914.

[32] M. Zahri, Multidimensional Milstein scheme for solving a stochastic model for prebiotic evolution, Journal of Taibah University for Science, Volume 8, Issue 2, April 2014, Pages 186-198.

[33] M. Zahri, Colored-Noise-Like Multiple Itô Stochastic Integrals: Algorithms and Numerics Journal of Numerical Mathematics and Stochastics, 7 (1): 48-69, 2015

[34] M. Zahri, Barycentric interpolation of interface-solution for solving stochastic partial differential equations on non-overlapping subdomains with additive multi-noises, International Journal of Computer Mathematics, Volume 95 (2018), Issue 4, Pages 645-685